# Supporting Online Material for

## Persistent Positive North Atlantic Oscillation Mode Dominated the Medieval Climate Anomaly

Valérie Trouet,* Jan Esper, Nicholas E. Graham, Andy Baker, James D. Scourse, David C. Frank

*To whom correspondence should be addressed. E-mail: trouet@wsl.ch

Published 3 April 2009, *Science* **324**, 78 (2009)
DOI: 10.1126/science.1166349

**This PDF file includes:**

# Supporting online material for Trouet, V., Esper, J., Graham, N.E., Baker, A., Scourse, J.D., and Frank, D.C., 'Persistent positive North Atlantic Oscillation mode dominated the Medieval Climate Anomaly'

## *Materials and Methods*

**Proxy records.** Analogous to instrumental NAO indices, $NAO_{ms}$ was calculated as the difference of a speleothem-based precipitation reconstruction (900-1993) (*S1*) and a tree-ring based drought reconstruction (1049-2002) (*S2*). Organic matter in an actively growing stalagmite from NW Scotland formed continuous, annual luminescent bands. Instrumental data comparisons demonstrated that growth rates were primarily controlled by precipitation variability and annual band width data were used accordingly to reconstruct winter precipitation. The second drought reconstruction was based on annual ring width measurements from 326 *Cedrus Atlantica* trees from four sites in the Atlas Mountains in Morocco. Detrending techniques to preserve inter-annual to multi-centennial variability in the tree-ring series were applied and the high sensitivity to water availability fluctuations allowed for reconstruction of February-June Palmer Drought Severity Index (PDSI) (*S3, S4*) variability. The annual precipitation reconstruction for Scotland and the PDSI reconstruction for Morocco, as well as their difference, correlated significantly with a principal component based time series (1901-2002) of seasonal SLP anomalies from the North Atlantic sector (*S5*) ($r=0.4$, $r=-0.31$, and $r=0.39$, respectively, all $p<0.01$).

**Low-pass filtering.** In order to determine the most appropriate smoothing for the reconstruction of long-term changes in the NAO, we calculated Pearson's correlation coefficients for averages within non-overlapping segments of the two proxy series for various segment lengths (Fig. S4). Correlations increased linearly with increasing segment length up to 20 years, then showed a steep jump, after which they stabilized again. With increasing segment length, the number of segments, and thus the degrees of freedom, decreases. At a segment length of 30 years, the degrees of freedom are reduced to 30 (corresponding to 32 non-overlapping segments), but the correlation coefficient of -0.71 is still significant ($p<0.01$). This approach of non-overlapping segments conservatively avoids uncertainties associated with determination for degrees of freedom with smoothed data (*S6*). Both records show substantial autocorrelation (Fig. S4), but on an annual scale it is considerably higher for the Scotland record than for the Morocco chronology ($r=0.88$ vs. $r=0.54$), due to the effects of groundwater mixing in the former, which preferentially preserves lower frequency climate information (*S7*). Lag1 autocorrelations of the records approach each other after 20-year smoothing with minimal changes at increasing window lengths. Thus, based on the correlation and the autocorrelation functions of both proxy series and dating uncertainties in the stalagmite record (*S1*), a 30-year smoothing spline was applied to the proxy data before differencing to $NAO_{ms}$.

**Error estimation.** The overall uncertainty of $NAO_{ms}$ is represented by the square root of three summed and squared individual error terms. These individual error terms include (i) dating uncertainties of the speleothem record, (ii) chronology error of the tree-ring record, and (iii) calibration error of the residual record $NAO_{ms}$.
Calendric accuracy of the speleothem record is hindered by dating uncertainties that lead to a maximum error of +/-20 years at ~1ka BP based upon a basal U-Th date assessment. No dating uncertainties occurred in the period after 1837 (*S1*). Considering that the effect of this uncertainty would be roughly equivalent to temporally shifting the time series by the dating error, uncertainties were conservatively estimated as running maxima and minima of the speleothem series with window lengths increasing linearly back in time from 1 in the year 1837 to 20 in the year 1000.
We estimated uncertainties related to the varying number of contributing tree-ring series back in time and to the variance of these series around the mean value function using bootstrap confidence intervals (*S2*). Available series for each year were sampled with replacement 1000 times and arithmetic means calculated. The empirical distribution of these 1000 bootstrap means for each year served as the basis for estimating two-tailed 95% confidence limits. The confidence limits include corrections for bias and skew, which provide second-order correctness.
Calibration uncertainty of $NAO_{ms}$ was estimated as two standard error (95%) confidence intervals derived from linear regression against the 30-year smoothed Ponta Delgada (*S8*) instrumental NAO series (1865-1995).

**PSR reconstruction.** PSR (*S9*) is a method for making proxy-guided multi-variate reconstructions from climate model data. Let P be an array of NP time series (length $NT_P$) of climate proxy data that correspond to output or derived variables from a climate model. Let M be an array of NP time series (length $NT_M$) of the corresponding climate data drawn from a climate model simulation. For each of the i = 1, $NT_P$ proxy "observations" ($P_i$) find the model output temporal index (j, in the range 1, $NT_M$) for which the similarity between $P_i$ and $M_j$ is maximized. In a reordering vector (O), set $O_i = j$, i.e., the model data from time index j is most similar to the proxy data from time index i. When all the $NT_P$ realizations have been so treated, O provides a reordering of the model data for which the model-proxy agreement at the NP proxy locations is maximized.
For the PSR analysis in this work, the Scotland speleothem record was transformed into precipitation (as fraction of modern climatology) using Lamb's documentary evidence-based estimate of a 13% MCA-to-LIA reduction in September-June England-Wales rainfall (*S10*). This record was compared with December-March precipitation from the CGCMs over the region 10W-5E and 54-60N. The MCA-to-LIA Scotland proxy precipitation reduction was reduced to about 8% to make it consistent with the reconstructed Morocco precipitation data (20% reductions in the MCA) and the Scotland-Morocco precipitation relationship seen in the CGCMs and documentary data (*S11*).
The Morocco PDSI reconstruction was calibrated using linear regression against smoothed (weighted average of December-January precipitation from the previous two years) observed regional average precipitation data for 1936-1995 (CRU version TS 2.1 (*S12*)). The correlation between the proxy and observed precipitation data over this period is 0.77. The reconstructed data were rescaled to match the variance of the smoothed observations

over the calibration period. The derived reconstruction indicates an MCA-to-LIA increase in Morocco winter precipitation of about 20%.

For Alps temperature, the smoothed (25-year running mean) Spannagel (*S13*) record was calibrated using linear regression against smoothed area-average (6-14E, 46-48N) December-February temperature from a documentary evidence-based data set (*S14, S15*) over the period 1525-1903. The correlation between these records is 0.69, with both time series showing four distinct peaks (see Fig. 4 in (*S13*)) over the calibration period. No rescaling was applied for this reconstruction. The resulting reconstruction gives an MCA-to-LIA winter temperature decrease in the Alps of approximately 0.4˚ C. The reconstructed temperature changes used here are considerably smaller than the approximately 1.2˚ C MCA-to-LIA decrease in centennial average annual temperature obtained using a different reconstruction method (*S13*). In the PSR analysis, this record was compared to smoothed CGCM December-March temperature anomalies for the region 6-16E, 45-50N.

The MCA-to-LIA winter precipitation increase for Morocco is reduced to approximately 15% if the proxy precipitation reconstruction is not rescaled (i.e., the regression coefficient is used directly). When variance-conserving rescaling is applied to the Alps temperature reconstruction (*S16*), the amplitudes of the four peaks in the historical record mentioned above are more closely matched, and the MCA-to-LIA winter temperature difference is approximately -0.6˚ C. Not surprisingly, changing the scaling details affects the amplitude of PSR-inferred MCA-to-LIA related climatic changes, but has little effect on the spatial patterns of change (Fig. 2B, Fig. S3C).

## *Supporting Text*

PSR field reconstructions are subject to the uncertainty inherent in i) the conversion of the proxy data to precipitation and temperature and ii) non-stationary relationships between climate variables and the NAO.

**Proxy to climate data conversion.** The Morocco and Alps proxy records calibrate well with available instrumental and historical/documentary data. The use of Lamb's England-Wales (EW) documentary-based precipitation record (*S10*) to calibrate the Scotland speleothem record in the PSR reconstructions is based on the close similarity between the two records. Correlations between annual December-March precipitation (unsmoothed, gridpoint values from CRU TS 2.1 data) (*S12*) and the NAO are highest along the western part of Great Britain and decrease from north to south. For example, over the 20$^{th}$ century the correlation between area-averaged annual winter Scotland precipitation and the NAO is 0.75, while for southern Britain (south from 54° N, EW) it is 0.17. These differences are reduced when the time series are smoothed. For 11-year running means, the correlation between Scotland precipitation and the NAO is 0.71, for EW it is 0.48. For 25-year smoothing, the Scotland-NAO correlation is 0.62 and 0.78 for EW. The smoothed records allow fewer degrees of freedom, but the 25-year smoothed NAO and precipitation series from both Scotland and EW show very similar "U-shaped" curves from positive values at the turn of the century to a minimum around 1970 and strongly increasing values after that. Comparing the Scotland and EW precipitation records with 25-year smoothing gives a maximum correlation of 0.80 at 1-year lag. With 25-year smoothing, the variability in Scotland precipitation (expressed as fraction of the long-term mean) is about 60% larger than in the EW record, implying that the actual MCA-to-LIA precipitation changes in Scotland might have been greater than the 8% used in the PSR reconstruction. This analysis indicates that for the 50-year averaging periods used in Lamb's EW reconstruction), both the NAO and Scotland precipitation should be reasonably well represented by area-average EW precipitation, though the magnitude of the inferred changes in precipitation in Scotland may be too small.

**Non-stationary NAO-climate teleconnections.** Noting that the difference between Scotland and Morocco precipitation is the key driver of the PSR reconstruction with respect to the NAO, we tested the stationarity of relationship between Scotland and Morocco precipitation difference (δP) and the NAO using NCAR CCSM (*S17)* and MPI coupled ECHAM4-OPYC (*S18)* model data. For the 1150-year CCSM data, δP-NAO regression coefficients (expressed as fractions of their mean value) calculated over 50-year windows have a standard deviation of 12% and full range of +30% to -20%. For the 240-year MPI data, the standard deviation of the regression coefficients amounts to 4% of the mean value, with a range of +12% to -8%. For the 20$^{th}$ century CRU data (*S12*) (and noting there are only two independent periods) the standard deviation of the regression coefficients amounts to 10% of the mean value and the full range is +25% to -10%.

These results suggest that non-stationarity in the δP-NAO relationship, a key driver of the PSR reconstructions for the NAO, will add a modest amount of additional uncertainty to changes in the NAO inferred from the PSR reconstructions.

*Supporting figures*

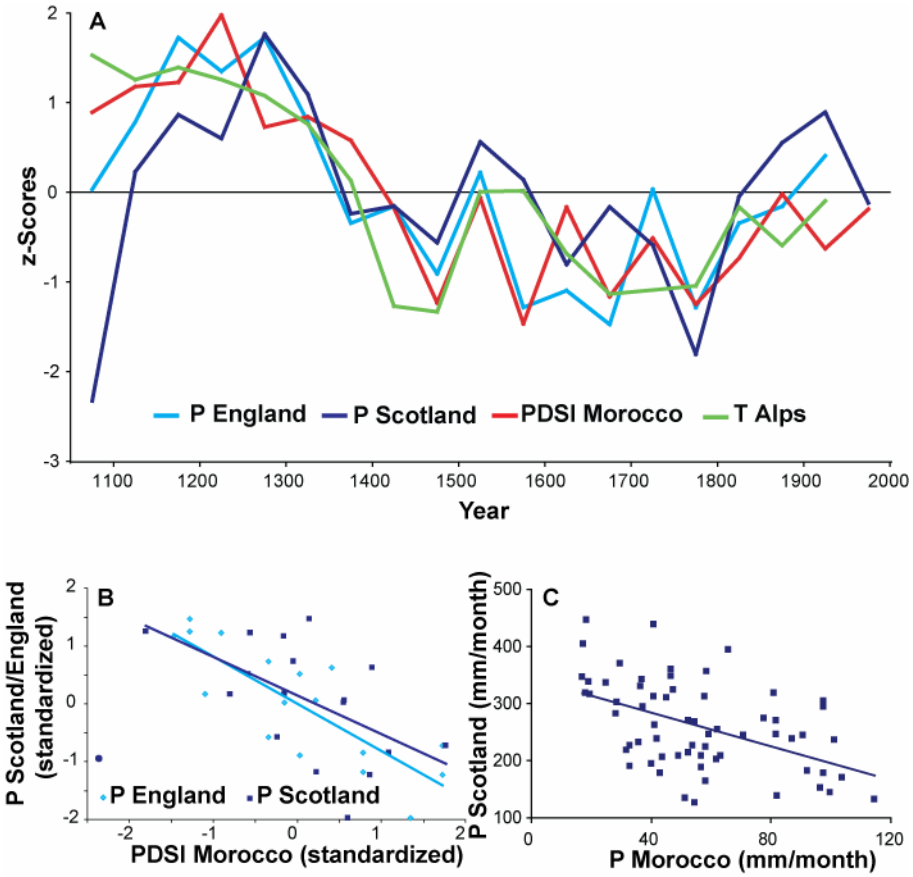


**Figure S1: Long-term winter proxy records from Europe.** Comparison of the tree-ring based Morocco (*S2*) and speleothem based Scotland (*S1*) records with a documentary based estimate of September-June England-Wales precipitation (*S10*) and speleothem based estimate of winter temperature from the central Alps (*S13*) (**A**). Time series consist of 25-year averages, standardized over the common period (1075-1925). The Morocco PDSI record was inverted. Panel **B** is a scatterplot of Morocco PDSI versus Scotland (dark blue; r=-0.56, p<0.01) and England (light blue; r=-0.82, p<0.01) precipitation data as shown in **A**. Dark blue dot indicates an outlier in the Morocco vs. Scotland plot. Panel **C** is the scatterplot of the annual instrumental CRU TS2.1 (*S12*) December-February precipitation data for a gridpoint in Morocco (5W-32.5N) versus a gridpoint in Scotland (5W-57.5N), calculated over the 1940-2002 period (r=-0.49, p<0.01).

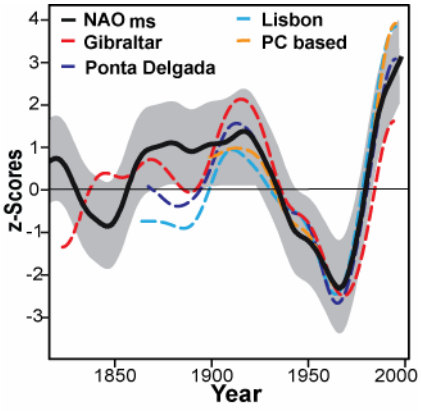


**Figure S2: Instrumental and proxy based NAO records from Europe.** Decadal-scale variability in $NAO_{ms}$, the station based Gibraltar-Iceland (*S19*) (Gibraltar), Ponta Delgada-Iceland (*S8*) (Ponta Delgada), and Lisbon-Iceland (*S5*) (Lisbon) indices, and the principal component based time series of seasonal SLP anomalies from the North Atlantic sector (*S5*) (PC based). All time series were smoothed using a 30-year spline and normalized over the common period (1899-1995). Pearson correlation coefficient between $NAO_{ms}$ and Ponta Delgada is 0.86 ($p<0.01$; $df=9$; 1865-1995).

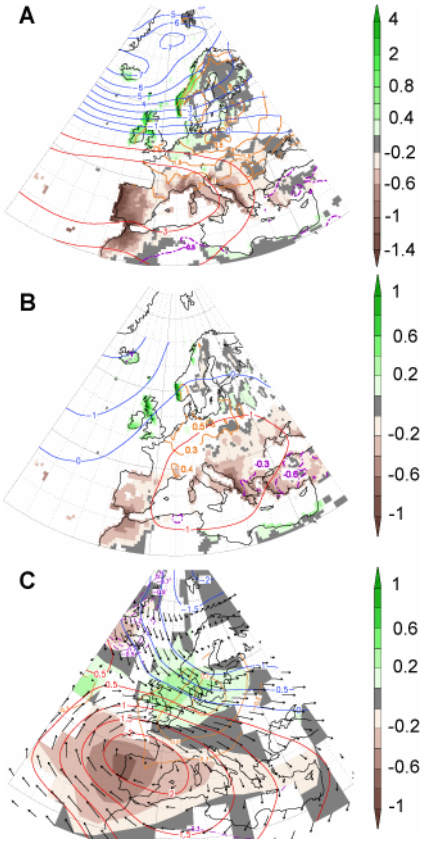


**Figure S3: Empirical and model derived NAO patterns.** Instrumental (*S12, S20*) (**A**), reconstructed (*S11, S14*) (**B**), and PSR (*S9*) estimated [using CCSM model (*S17)* data] (**C**) fields of December-February SLP, temperature, and precipitation are composited for positive and negative NAO phases. NAO phases were determined in (**A**) as the 50% most positive and the 50% most negative NAO (*S5*) winters (1901-2000), in (**B**) as the 33% most positive versus the 33% most negative $NAO_{ms}$ winters (1659-1995; Fig. 1) and in (**C**) as the average values for the period 1049-1298 minus those for 1448-1923. Composite difference maps are shown for SLP (red and blue contours; in meters), temperature (orange and dashed purple contours; in ˚ C), and precipitation (shaded areas; in mm). Shaded areas and contours reflect significant ($p<0.1$) differences, calculated using a t-test.

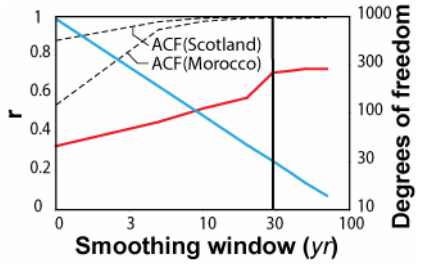


**Figure S4: Frequency-dependent correlation statistics of the Scotland and Morocco proxy records**. Pearson correlation coefficients for Morocco (*S2*) vs. Scotland (*S1*) (red), lag1 autocorrelation coefficients (ACF) for the individual records (dashed), and number of degrees of freedom (blue) plotted as a function of increasing smoothing window length. Correlations were computed for a continuum between unfiltered data and low-pass spline filters with 50% frequency-response thresholds up to 75 years. The smoothing window axis and the degrees of freedom axis are log scaled. 30-year smoothing (vertical black line) was chosen based on the balance between these three functions and considerations of dating uncertainties in the stalagmite record (*S1*).

*Supporting tables*

**Table S1**: **Correlation between NAO reconstructions** (*S21-S23)*. All reconstructions were smoothed using a 30-yr spline. Pearson correlation coefficients for the Luterbacher reconstruction were calculated for three periods (1500-1658, 1659-1823, and 1824-1995).

| | **$NAO_{ms}$** | **Cook** | **Glueck** | **Luterbacher 1500-1658** | **Luterbacher 1659-1823** | **Luterbacher 1824-1995** |
|---|---|---|---|---|---|---|
| **$NAO_{ms}$** | | 0.58 | 0.47 | 0.29 | 0.51 | 0.67 |
| **Cook** | | | 0.4 | 0.24 | 0.67 | 0.8 |
| **Glueck** | | | | -0.39 | 0.31 | 0.49 |

**Table S2: Type and climate signal for the proxy records referred to in Figure 4**

| | Designation | Proxy type | Climate signal | Source |
|---|---|---|---|---|
| **European temperature** | Aletsch | Glacier mass balance | Glacier fluctuation, temperature | Holzhauser *et al*. 2005 (*S24*) |
| | LCT | Documentary data | winter temperature | Shabalova and Van Engelen 2003 (*S25*) |
| | Lötschental | Tree-ring (latewood density) | summer temperature | Büntgen *et al*. 2006 (*S26*) |
| | Spannagel | Stalagmite ($\delta^{18}O$) | winter temperature | Mangini *et al.* 2005 (*S13*) |
| **North Atlantic** | Bermuda Rise | Coral $\delta^{18}O$ | SST | Keigwin 1996 (*S27*) |
| | Cape Ghir | Marine core (alkenones) | SST, coastal upwelling | McGregor *et al*. 2007 (*S28*) |
| | Florida Strait | Marine core (foraminifera) | Gulf stream transport | Lund *et al.* 2006 (*S29*) |
| | Iceland | Marine core (alkenones) | SST | Sicre *et al.* 2008 (*S30*) |
| | Cariaco Basin | Marine core (Titanium) | Precipitation, run-off | Haug *et al*. 2001 (*S31*) |
| **Tropical Pacific** | Palmyra | Coral $\delta^{18}O$ | SST | Cobb *et al.* 2003 (*S32*) |
| | Mindanao | Marine core (foraminifera) | SST | Stott *et al.* 2004 (*S33)* |
| | Aculeo | Lake core | Cool-season precipitation, | Jenny *et al.* 2002 |

| | | | |
|---|---|---|---|
| | (multiproxy) | inflow | (*S34*) |
| Western USA | Tree-rings (ring width) | cool-season precipitation | Cook *et al*. 2004 (*S35*) |
| Naivashi | Lake core (salinity) | Lake level, precipitation | Verschuren *et al*. 2000 (*S36*) |
| Peru | Marine core (lithics) | River flow | Rein *et al.* 2004 (*S37*) |

## *Supporting references*


S1. C.J. Proctor, A. Baker, W.L. Barnes, R.A. Gilmour, *Clim. Dyn.* **16**, 815 (2000).
S2. J. Esper *et al.*, *Geophys. Res. Lett*. **34**, doi: 10.1029/2007GL030844 (2007).
S3. W.C. Palmer, "Meteorological Drought" (Research paper 45, U.S. Dept. of Commerce, Washington, DC, 1965).
S4. A.G. Dai, K.E. Trenberth, T.T. Qian, *J. Hydromet.* **5**, 1117 (2004).
S5. J.W. Hurrell, *Science* **269**, 676 (1995).
S6. T.J. Osborn, K.R. Briffa, *Dendrochronologia* **18**, 9 (2000).
S7. M. Tan *et al.*, *Quat. Sci. Rev.* **25**, 2103 (2006).
S8. J.C. Rogers, *Mon. Weath. Rev.* **112**, 1999 (1984).
S9. N.E. Graham, *Clim. Change* **83**, 241 (2007).
S10. H.H. Lamb, *Palaeogeogr, Palaeoclim. Palaeoecol.* **1**, 13 (1965).
S11. A. Pauling, J. Luterbacher, C. Casty, H. Wanner, *Clim. Dyn.* **26**, 387 (2006).
S12. T.D. Mitchell, T.R. Carter, P.D. Jones, M. Hulme, M. New, "A Comprehensive Set of High-resolution Grids of Monthly Climate for Europe and the Globe: the Observed Record (1901-2000) and 16 Scenarios (2001-2100)" (Working Paper 55, Tyne Centre for Climate Change Research, University of East Anglia, Norwich, 2004).
S13. A. Mangini, C. Spotl, P. Verdes, *Earth Planet. Sci. Lett.* **235**, 741 (2005).
S14. J. Luterbacher *et al*., *Clim. Dyn.* **18**, 545 (2002).
S15. C. Casty, H. Wanner, J. Luterbacher, J. Esper, R. Böhm, *I. J. Climatol.* **25**, 1855 (2005).
S16. J. Esper, D.C. Frank, R.J.S. Wilson, K.R. Briffa, *Geophys. Res. Lett.* **32**, doi: 10.1029/2004GL021236 (2005).
S17. C.M. Ammann, F. Joos, D.S. Schimel, B.L. Otto-Bliesner, R.A. Tomas, *Proc. Natl. Acad. Sci. U.S.A.* **104**, 3713 (2007).
S18. E. Roeckner, L. Bengtsson, J. Feichter, J. Lelieveld, H. Rodhe, *J. Clim.* **12**, 3004 (1999).
S19. P.D. Jones, T. Jonsson, D. Wheeler, *I. J. Climatol.* **17**, 1433 (1997).
S20. K.E. Trenberth, D.A. Paolino, *Mon. Weath. Rev.* **108**, 855 (1980).
S21. E.R. Cook, R.D. D'Arrigo, M.E. Mann, *J. Clim.* **15**, 1754 (2002).
S22. M.F. Glueck, C.W. Stockton, *I. J. Climatol.* **21**, 1453 (2001).
S23. J. Luterbacher, C. Schmutz, D. Gyalistras, E. Xoplaki, H. Wanner, *Geophys. Res. Lett.* **26**, 2745 (1999).
S24. H. Holzhauser, M. Magny, H.J. Zumbuhl, *Holocene* **15**, 789 (2005).
S25. M.V. Shabalova, A.G.V. van Engelen, *Clim. Change* **58**, 219 (2003).
S26. U. Büntgen, D.C. Frank, D. Nievergelt, J. Esper, *J. Clim.* **19**, 5606 (2006).
S27. L.D. Keigwin, *Science* **274**, 1504 (1996).
S28. V. McGregor, M. Dima, H.W. Fischer, S. Mulitza, *Science* **315**, 637 (2007).
S29. D.C. Lund, J. Lynch-Stieglitz, W.B. Curry, *Nature* **444**, 601 (2006).
S30. M.A. Sicre *et al*., *Earth Planet. Sci. Lett.* **268**, 137 (2008).
S31. G.H. Haug, K.A. Hughen, D.M. Sigman, L.C. Peterson, U. Rohl, *Science* **293**, 1304 (2001).
S32. K.M. Cobb, C.D. Charles, H. Cheng, R.L. Edwards, *Nature* **424**, 271 (2003).

S33. L.D. Stott *et al.*, *Nature* **431**, 56 (2004).
S34. B. Jenny *et al., Quat. Res.* **58**, 160 (2002).
S35. E.R. Cook, C.A. Woodhouse, C.M. Eakin, D.M. Meko, D.W. Stahle, *Science* **306**, 1015 (2004).
S36. D. Verschuren, K.R. Laird, B.F. Cumming, *Nature* **403**, 410 (2000).
S37. B. Rein, A. Luckge, F. Sirocko, *Geoph. Res. Lett.* **31**, L17211 (2004).